A&A 398, 127–132 (2003)
DOI: 10.1051/0004-6361:20021696

Astronomy & Astrophysics

Massive $z \sim 1.3$ evolved galaxies revealed⋆

P. Saracco[1], M. Longhetti[1], P. Severgnini[1], R. Della Ceca[1], F. Mannucci[2], R. Bender[3], N. Drory[4], G. Feulner[3], F. Ghinassi[5], U. Hopp[3], and C. Maraston[3]

[1] INAF - Osservatorio Astronomico di Brera, Via Brera 28, 20121 Milano, Italy
e-mail: [saracco, marcella]@merate.mi.astro.it; [paola, rdc]@brera.mi.astro.it
[2] IRA-CNR, Largo E. Fermi 5, 50125 Firenze, Italy
e-mail: filippo@arcetri.astro.it
[3] Universitäts-Sternwarte München, Scheiner Str. 1, 81679 München, Germany
e-mail: [bender, feulner, hopp, maraston]@usm.uni-muenchen.de
[4] University of Texas at Austin, Austin, Texas 78712, USA
e-mail: drory@astro.as.utexas.edu
[5] Centro Galileo Galilei, La Palma, Spain
e-mail: ghinassi@tng.iac.es

Received 19 September 2002 / Accepted 8 November 2002

Abstract. We present the results of TNG near-IR low resolution spectroscopy of two (S7F5_254 and S7F5_45) sources belonging to a complete sample of 15 EROs with $K' < 18$ and $R - K' > 5$ selected from the MUNICS Survey. Both the spectra show a sharp drop in the continuum which can be ascribed only to the Balmer break. This places them at $1.2 < z < 1.5$. Their rest-frame $z = 1.2$ K-band absolute magnitude is $M_K \simeq -26.6$ ($L \sim 7L^*$). The comparison of the spectra and the photometric data with a grid of synthetic template spectra provides a redshift $z \simeq 1.22^{-0.07}_{+0.2}$ for S7F5_254 and $z \simeq 1.46 \pm 0.02$ for S7F5_45. The resulting lower limits to their stellar mass are $\mathcal{M}^{\rm min}_{\rm stars} = 6 \times 10^{11}\ M_\odot$ and $\mathcal{M}^{\rm min}_{\rm stars} = 4 \times 10^{11}\ M_\odot$. The minimum age of the last burst of star formation in S7F5_254 is 3.5 Gyr while it is 0.5 Gyr in S7F5_45 implying a minimum formation redshift $z_{\rm f} \gtrsim 3.5$ and $z_{\rm f} \gtrsim 2$ for the two EROs respectively.

Key words. galaxies: evolution – galaxies: elliptical and lenticular, cD – galaxies: formation

1. Introduction

The existence of massive (e.g. $\mathcal{M}_{\rm stars} > 10^{11}\ M_\odot$) galaxies at $z > 1$ and their spatial density provide crucial constraints on the current galaxy formation and evolution models. The current ΛCDM hierarchical merging scenario predicts, indeed, that massive galaxies are assembled by means of subsequent mergers of disk galaxies largely occurring at $z < 1.5$ (e.g. Kauffmann 1996; Cole et al. 2000; Baugh et al. 2002). In this scenario the higher the stellar mass of galaxies, the lower is the probability of their existence at increasing redshift. For instance, the predicted space density of $\mathcal{M}_{\rm stars} > 10^{11}\ M_\odot$ galaxies is $<10^{-5}h^3$ Mpc^{-3} at $z \sim 1$, i.e. <0.02 galaxies arcmin^{-2} at $1.2 < z < 1.5$ ($h = 0.7$) (Baugh et al. 2002). An alternative scenario is the "monolithic collapse" where, in the traditional form, even the most massive galaxies formed at $z_{\rm f} \gtrsim 3$ from the collapse of proto-galactic gas clouds. Almost all of their stellar mass is produced in a single short episode of star formation. Their evolution should then follow a passive aging (Tinsley 1977; Bruzual & Kron 1980) as suggested by the observed properties of local spheroids (e.g. Renzini & Cimatti 1999; Peebles 2001; for recent reviews). A modern and more realistic view of the single-collapse model predicts that the star formation in elliptical galaxies lasts longer than 10^8 yr (e.g. Jimenez et al. 1999). In this scenario the spatial density of massive evolved galaxies is almost constant over a wide redshift range ($0 < z < z_f$). This is the main reason why in the last few years, the search for $z > 1$ massive galaxies has been attempted. Samples of candidates of evolved galaxies at $z > 1$ have been selected on the basis of optical-IR colors (e.g. $R - K > 5$), the so called Extremely Red Objects (EROs; e.g. Thompson et al. 1999; Scodeggio & Silva 2000; Daddi et al. 2000; McCarthy et al. 2001; Martini 2001; Roche et al. 2002). Because of the age-dust degeneracy, both $z > 1$ old stellar systems and dusty star forming objects spanning a wider range of redshift can populate the ERO regime in color space (Cimatti et al. 1999; Dey et al. 1999; Mannucci et al. 2002). The recent estimates by Cimatti et al. (2002), based on optical spectroscopy of a complete sample of $K \leq 20$ galaxies over 50 arcmin^2 and by Mannucci et al. (2002) based on the color-color diagram,

Send offprint requests to: P. Saracco,
e-mail: saracco@merate.mi.astro.it

⋆ Based on observations carried out at the Italian Telescopio Nazionale Galileo (TNG, www.tng.iac.es).

show that the two classes are about equally populated and that a substantial population of passively evolved galaxies at $z \sim 1$ exists (see also Franceschini et al. 1998). At higher redshift ($z > 1$), where the two paradigms of galaxy formation could be better distinguished, the existence of massive and/or evolved galaxies has not yet been proved. The detection of a massive disk galaxy at $z = 1.3$ by van Dokkum & Stanford (2001) could cast doubts on the current hierarchical models since they do not predict such regular, massive disk systems at $z > 1$. However, it could be an exceptional case. Evolved galaxies have been discovered at $z \geq 1.5$ (Soifer et al. 1999; Benitez et al. 1999; Stiavelli et al. 1999) but their small stellar masses do not provide severe constraints.

The search for massive evolved galaxies at $z > 1$ needs both a wide angle K-band survey and spectroscopy in the near-IR. Indeed, the expected apparent magnitude of a $\mathcal{M}_{\rm stars} > 10^{11}\ M_{\odot}$ galaxy at $1 < z < 1.5$ is $K \sim 18 - 18.5$ (e.g. Kauffmann & Charlot 1998). The observed surface density of $K \leq 18$ EROs is 0.05–0.1 arcmin^{-2} (e.g. Daddi et al. 2000) and about half of them can be dusty galaxies (Cimatti et al. 2002). Thus, a reasonable probability to find $z > 1$ massive evolved galaxies can be achieved over areas larger than few hundreds arcmin^2. Moreover, spectroscopy in the near-IR is needed to make possible the detection of the 4000 Å break at these redshifts.

In this paper we report the analysis of two $K' < 18.0$ unlensed EROs spectroscopically observed in the near-IR as a part of the ongoing project TESIS (TNG EROs Spectroscopic Identification Survey; Saracco et al. 2002), aimed at searching for $\mathcal{M}_{\rm stars} > 10^{11}\ M_{\odot}$ evolved galaxies at $z > 1$. Throughout this paper we assume $H_0 = 65$ km s^{-1} Mpc^{-1}, $\Omega_0 = 0.3$ and $\Lambda_0 = 0.7$.

2. Observations and data reduction

The two EROs presented here belong to a complete sample of 15 candidates massive $z > 1$ evolved galaxies selected from two no-adjacent areas of about 180 arcmin^2 each from the Munich Near-IR Cluster Survey (MUNICS; Drory et al. 2001). The sample includes all the galaxies redder than $R - K' = 5$ corresponding to a surface density of EROs of 0.04 arcmin^{-2} at $K' < 18$. In Table 1 the relevant photometric information for the two targets is summarized. The two EROs are placed in a high Galactic latitude field selected to contain no bright galaxies or known nearby clusters of galaxies. We visually inspected the K-band image without finding any candidate lensing objects. Thus, we are confident that the magnitudes of the two EROs are not affected by magnification of foreground massive objects.

Spectroscopic observations, carried out during the night of March 6 2002 with 1.″5 wide slit, are based on the Amici prism dispersing element (Oliva 2001) mounted at the near-IR camera NICS of the Italian 3.6 m Telescopio Nazionale Galileo (TNG). The Amici prism provides the spectrum from 0.85 μm to 2.4 μm in one shot with a nearly constant spectral resolution of $\Delta\lambda/\lambda \sim 50$ (1″ slit) over the whole spectral range. This results in a dispersion of ∼30 Å (100 Å) per pixel and a full-width at half-maximum ($FWHM$) of ∼200 Å (∼400 Å) at 10 000 Å (20 000 Å). This very low-resolution mode is best suited to detect continuum breaks resulting very efficient in identifying old stellar systems at $z > 1.2$. The targets were acquired by means of a nearby brighter reference object put in the slit. Dithering of the targets along the slit in a A-B-B-A pattern with small offset about each of the two positions were used. Integrations of 2 min for each exposure were adopted for all the observations in order to be background limited in K' band. A total integration time of ∼100 min for each source was accumulated.

After the sky subtraction, the frames have been aligned and co-added. Wavelength calibration was performed using the deep telluric absorption features. The telluric absorptions were then removed by dividing each of the object spectra by an A0 reference star spectrum taken at similar airmass and adjacent in time. The intrinsic features and shape of the reference star were then removed by multiplying the spectrum by a synthetic A0 star spectrum smoothed to the appropriate resolution.

The final extracted spectra of S7F5-45 and S7F5-254 are shown in Fig. 1 (upper panel and lower panel respectively) along with the relevant mean sky residuals. Filled symbols are the photometric data in the I, J and K' bands (see Table 1) from the MUNICS survey (Drory et al. 2001). The spectra are normalized to the K-band flux. As an independent check on the near-IR photometry, we derived a flux calibration of the spectra by comparing the mean count rate at K in the targets to the mean count rate of the A0 star whose K magnitude is known (Hunt et al. 2000). For both the EROs the flux density we inferred from the spectra matches the near-IR photometry of the MUNICS catalog within a factor of 1.3 in flux.

3. Analysis of the Amici spectra

In the following sections we analyze the Amici spectral data. We derive the redshift range of the two galaxies from their continuum shape and an estimate of their stellar mass based on their K-band luminosity and on the mean local mass-to-light ratio.

3.1. Redshift estimate

The spectra of both the EROs are almost flat at wavelength $\lambda > 1.0$ μm and drop rapidly below this wavelength. We do not detect any emission feature and we estimate a limiting equivalent-width (EW) for the emission line detection of ∼125 Å and ∼150 Å in the J band for S7F5_45 and S7F5_254 respectively. The only continuum feature is the change of the slope at $\lambda < 1.0$ μm where the continuum flux drops by a factor of 4 at $\lambda \sim 0.9$ μm. We rule out the possibility that the break is due to the Lyman-limit because of the detection of both the galaxies in the V and R bands. It is worth noting that the broad band colors of S7F5_45 could be still compatible, even if marginally, with a high redshift ($z \sim 6$) galaxy (for instance an SB2 starburst galaxy from Kinney et al. 1996), given the large errors in the optical magnitudes. However, in this case, the shape of the near-IR spectrum rules out this hypothesis being it not compatible with that of any galaxy at such high redshift. Dust reddening produces smooth spectra (e.g. Schmitt et al. 1997) as it is almost inversely proportional to the

Table 1. Photometry of the two EROs S7F5_45 and S7F5_254 from the MUNICS catalog. All magnitudes are in the Vega system and measured within 5″ diameter aperture (Drory et al. 2001).

Object	RA(J2000)	Dec(J2000)	V	R	I	J	K
S7F5_254	13 34 59.6	16 49 10.7	25.4 ± 1.2	24.4 ± 0.5	23.1 ± 0.7	19.8 ± 0.1	17.8 ± 0.2
S7F5_45	13 34 25.0	16 45 48.6	24.2 ± 0.4	23.5 ± 0.3	22.2 ± 0.3	19.6 ± 0.1	17.65 ± 0.08

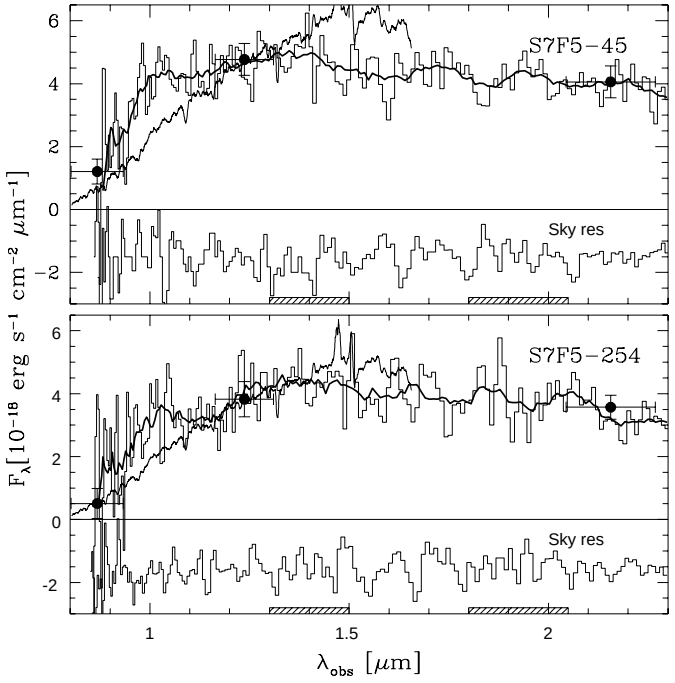

Fig. 1. *Upper panel*: NICS-Amici low resolution spectrum of the ERO S7F5_45 (thin histogram). The thick histogram is the spectrum heavily smoothed to show the continuum. The spectrum is normalized to the flux in the K-band. The shaded areas represent the atmospheric windows characterized by an opacity larger than 80%. The filled symbols are the photometric data in the I, J and K' bands from the MUNICS survey (Drory et al. 2001). The thin line is the optical spectrum of Arp220 redshifted at $z = 1.2$ and normalized to the J-band flux. The lower histogram is the mean sky residual (with an offset $-1.5{\times}10^{-18}$ erg cm^{-2} s^{-1} Å^{-1}) extracted above and below of the target spectrum. *Lower panel*: NICS-Amici low resolution spectrum of the ERO S7F5_254. Symbols are as in the upper panel.

wavelength: there is no way to produce a sharp break in the continuum like the one seen at $0.9 < \lambda < 1.0\,\mu$m in our spectra (see also Sect. 4). Thus, we identify the detected break as the 4000 Å break produced by the G and K stars. This places the two EROs at redshift $1.2 \leq z \leq 1.5$ and defines them as possibly early-type galaxies. It is worth noting that using the color-color diagnostic diagram suggested by Pozzetti & Mannucci (2000) both the EROs would lie on the elliptical side of the $(J-K)-(R-K)$ plane. For comparison, in Fig. 1 (thin line) the optical spectrum of Arp220 (UZC; Falco et al. 1999) redshifted at $z = 1.2$ is superimposed to the Amici spectra.

The spectra shown in Fig. 1 are comparatively different. The drop in the observed flux is sharper in S7F5_45 than in S7F5_254 and it is well constrained at $0.9 < \lambda < 1.0\,\mu$m. On the contrary S7F5_254 shows a first smooth decrease of the flux at $< 1.0 < \lambda < 1.3\,\mu$m followed by the drop which extends at $\lambda < 0.9\,\mu$m. These features suggest a redshift of S7F5_254 slightly lower than that of S7F5_45 and are typical of old stellar populations.

3.2. Luminosity and stellar mass estimate

In order to obtain a lower limit to the luminosity of the two galaxies and a model independent estimate of their stellar mass, we conservatively placed both of them at $z = 1.2$. Using a k-correction $\Delta K = -0.6$ mag (Mannucci et al. 2001) we estimate a lower limit to their rest-frame K-band absolute magnitude of $M_K \simeq -26.6$ mag. Cole et al. (2001) find $M^*_K = -24.4$ mag (scaled to $H_0 = 65$ km s^{-1} Mpc^{-1}) for the local luminosity function of galaxies. Thus, the luminosity of the two EROs is $L \sim 7L^*$. The brightest galaxies in the sample of Cimatti et al. (1999) have luminosities lower than L^* while the candidate old galaxy Cl 0939+4713B revealed by Soifer et al. (1999) has a luminosity comparable to those of our targets if the possible magnification induced by the foreground cluster is neglected. *Thus, the two EROs presented here are among the most luminous and, possibly, the most massive evolved galaxies detected so far at $z > 1$.* If we assume the local mean stellar mass-to-light ratio obtained by Cole et al. (2001) with the Kennicut IMF ($0.73\ M_\odot/L_\odot$) we derive a stellar mass for the two EROs $\mathcal{M}_{\rm stars} \simeq 7 \times 10^{11}\ M_\odot$ which would exceed $10^{12}\ M_\odot$ if we assume the $\mathcal{M}_{\rm stars}/L$ they derived with the Salpeter IMF ($1.32\ M_\odot/L_\odot$). However, these mean mass-to-light ratios are relevant to local galaxies. Higher redshift galaxies, on average younger than the local ones, should be described by lower ratios. This is quantitatively shown in Fig. 2 where the K-band stellar mass-to-light ratio as a function of age is shown for different initial mass functions (IMF; upper panel) and for different star formation histories and metallicity (lower panel).

4. Comparison with population synthesis models

In this section we analyze the two galaxies in more detail adding to the spectral information the available broad-band optical and near-IR photometry. The aim of this analysis is to obtain a more accurate estimate of the redshift of the two EROs and to set a lower limit to their stellar mass. To this end we constructed a grid of templates derived from the spectrophotometric models of Charlot & Longhetti (2001), based on the latest version of the Bruzual & Charlot (1993) population synthesis code. The grid constructed takes into account different star formation histories (SFH), metallicity and extinction. The parameters of the models are summarized in Table 2. The star formation histories considered, beside the simple stellar population (SSP) and the constant star formation (*cst*), are described by an exponentially declining SFR with an e-folding time τ. For each star formation history a set of 51 synthetic templates

Table 2. Parameters used to construct the grid of models.

SFH τ [Gyr]	0.1, 1, 2, 3, 5, 15, SSP, *cst*
Metallicity	0.2 $Z_\odot$, 0.4 $Z_\odot$, $Z_\odot$, 2 $Z_\odot$
A_V [mag]	0÷6 (step of 0.25 mag)
Extinction law	Calzetti et al. (2000)

in the range 10^6–1.5×10^{10} yr was generated with a Salpeter IMF (0.1 $M_\odot < \mathcal{M} < 100\ M_\odot$). By varying the metallicity, the star formation history and the extinction we built-up a grid of about 38 000 templates.

The redshift of the two EROs was formally measured by fitting the drop in the observed low resolution near-IR spectra beside the available optical and near-IR photometric data. The drop in the observed spectra has been described by four additional photometric points derived from the observed spectra in the wavelength range $0.9 < \lambda < 1.2\ \mu$m. Another additional photometric point has been derived in the H-band. Practically, we convolved the flux calibrated spectra with four rectangular 0.1 μm wide filters centered at $\bar{\lambda}_1 = 0.95\ \mu$m, $\bar{\lambda}_2 = 1.0\ \mu$m, $\bar{\lambda}_3 = 1.08\ \mu$m, $\bar{\lambda}_4 = 1.15\ \mu$m respectively and one 0.2 μm wide filter centered at $\bar{\lambda}_5 = 1.65\ \mu$m. The absolute calibration of the filters were derived by convolving them with the spectrum of an A0 star. We used the software *hyperz* (Bolzonella et al. 2000) to obtain the best fit to the 10 photometric points for each of these models.

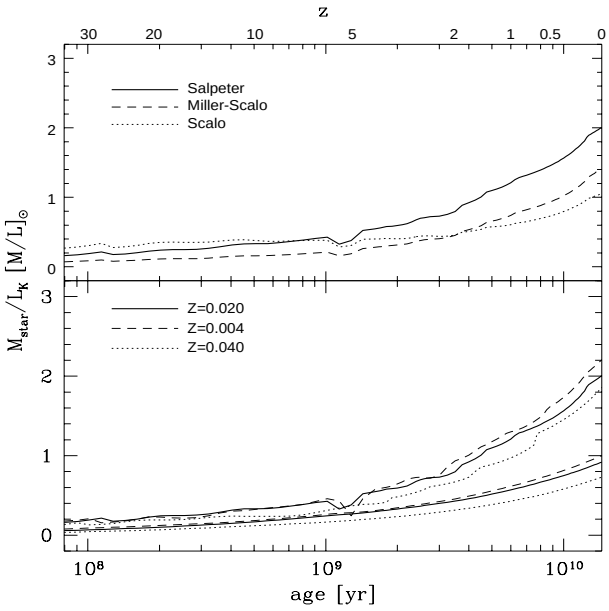

Fig. 2. *Upper panel*: mass-to-light ratio as a function of age for different IMF and a star formation history described by a SSP. *Lower panel*: mass-to-light ratio as a function of age for Salpeter IMF, different metallicity and a star formation history described by SSP (upper curves) and by *cst* (lower curves).

S7F5_254 - The best-fit value to the redshift of S7F5_254 is $z_{\rm best} = 1.22^{-0.07}_{+0.2}$ with a minimum reduced $\tilde{\chi}^2 = 0.35$ ($P(\tilde{\chi}^2) \simeq 0.96$). The quoted errors are not the uncertainties in the fit. They represent the boundary of the redshift range spanned by the statistically acceptable fit ($P(\tilde{\chi}^2) \geq 0.68$) obtained with the different models. This is shown in Fig. 3 where the best-fit value to the redshift as a function of the relevant $\tilde{\chi}^2$ is plotted for those models providing a statistically acceptable fit.

Formally, the best-fit to S7F5_254 data is given both by a 10 Gyr old SSP and a 10 Gyr old $\tau = 0.1$ model with $Z = Z_\odot$ and $A_V = 0$ (see Table 3). All the solar and sub-solar metallicity models with $\tau \leq 3$ provide a good fit ($P(\tilde{\chi}^2) > 0.9$) invoking very old stellar population (>10 Gyr) while none of them provide an acceptable fit with younger ages. Of course, this does not make sense since these ages are much larger than the Hubble time at $z \sim 1.2$. By forcing galaxies to have ages lower than the Hubble time at this z the only good result is obtained with $Z = 2\ Z_\odot$ models which provide a good fit to the data in the case of a 3.5 Gyr old $\tau = 0.1$ ($P(\tilde{\chi}^2) \simeq 0.95$) with an extinction $A_V = 0$. This is the youngest mean age we were able to obtain. It is worth noting that these properties are also displayed by the reddest early type cluster members at $z \sim 1.2$ (Rosati et al. 2000). The best fitting model parameters are summarized in Table 3 together with the 2nd best set of results. In Fig. 4 the best-fitting model, the observed spectrum and the photometric data relevant to S7F5_254 are shown (upper panel). For comparison, in the lower panel, we have superimposed to the data the mean observed spectrum of local ellipticals by Mannucci et al. (2001, Man01). The remarkable agreement is indicative once again for the old age of this galaxy. To derive a lower limit to the stellar mass we consider the youngest population model consistent with the data, i.e. the 3.5 Gyr $\tau = 0.1$ model. The lowest M/L ratio describing a stellar population 3.5 Gyr old fitting the data is ~0.4 $M_\odot/L_\odot$, obtained with the Scalo and Miller-Scalo IMFs. Since the K-band absolute magnitude of S7F5_254 resulting from the fitting models is $M_K = -27.08$ we derive a minimum stellar mass $\mathcal{M}^{\rm min}_{\rm stars} = 6\times10^{11}\ M_\odot$, where we have used $M_{\odot,K} = 3.4$ (Allen 1973). Being the $\tau = 0.1$ the youngest model, it requires the lowest formation redshift, $z_{\rm f}$, to fit the data. Indeed, any other exponentially decaying burst model would require star formation to have begun at a larger redshift. Thus, given the redshift of S7F5_254, the youngest best-fitting model requires for this galaxy a formation redshift $z_{\rm f} \gtrsim 3.5$.

S7F5_45 - The best-fit value to the redshift of S7F5_45 is $z_{\rm best} = 1.46 \pm 0.02$ ($\tilde{\chi}^2 = 0.33$, $P(\tilde{\chi}^2) \simeq 0.97$). Also in this case this value is matched by all the models providing a statistically acceptable fit ($P(\tilde{\chi}^2) \geq 0.68$) as shown in Fig. 3. In agreement with the results obtained in Sect. 3.1, S7F5_45 has a redshift higher than S7F5_254.

For this galaxy all the exponentially $\tau > 0.1$ decaying models do not provide acceptable fit to the data ($P(\tilde{\chi}^2) \ll 0.68$). The single-burst models provide good fit independently on the assumed metallicity. The best-fitting model is the $Z = 0.4\ Z_\odot$ single-burst, 0.5 Gyr old and with an extinction $A_V = 1.5$ mag (see Table 3). All the other SSP with different metallicities provide good fit as well ($0.93 < P(\tilde{\chi}^2) \leq 0.96$) giving mean ages in the range 0.25 Gyr ($Z = 2\ Z_\odot$) and 0.7 Gyr ($Z = 0.2\ Z_\odot$) and an extinction $1.25 \leq A_V \leq 1.5$. Only the $\tau = 0.1$ ($Z = Z_\odot$) is the exponentially decaying model providing a

Table 3. Parameters resulting from the best fits of stellar population models to the near-IR spectra and photometric data.

ERO ID	SFH	$\tilde{\chi}^2$	$P(\tilde{\chi}^2)$	z	Age (Gyr)	A_V (mag)	Z ($Z_\odot$)	M_K (mag)	$\mathcal{M}_{\rm stars}/L$ ($M_\odot/L_\odot$)	$\mathcal{M}_{\rm stars}$ (10^{11} $M_\odot$)
Best Fit										
S7F5_254	$\tau = 0.1$, SSP	0.35	0.96	1.22	10	0	1	−27.05	1.26	19
S7F5_45	SSP	0.33	0.97	1.46	0.5	1.5	0.4	−27.69	0.4	10
2nd Choice										
S7F5_254	$\tau = 0.1$	0.36	0.95	1.22	3.5	0	2	−27.08	0.46	7
S7F5_45	$\tau = 0.1$	0.37	0.95	1.45	0.5	1.75	1	−27.73	0.3	8

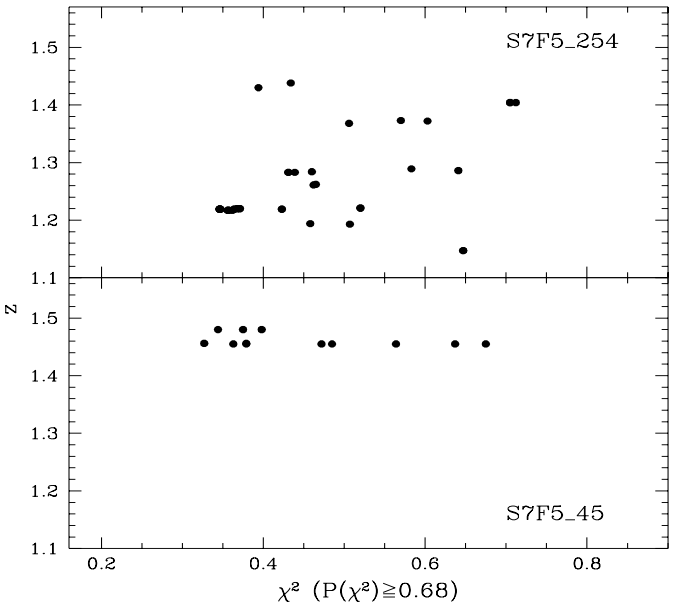

Fig. 3. Best-fit value to the redshift of S7F5_254 (upper panel) and of S7F5_45 (lower panel) as a function of the relevant reduced χ^2 for all the models providing a statistically acceptable fit ($P(\tilde{\chi}^2) \geq 0.68$).

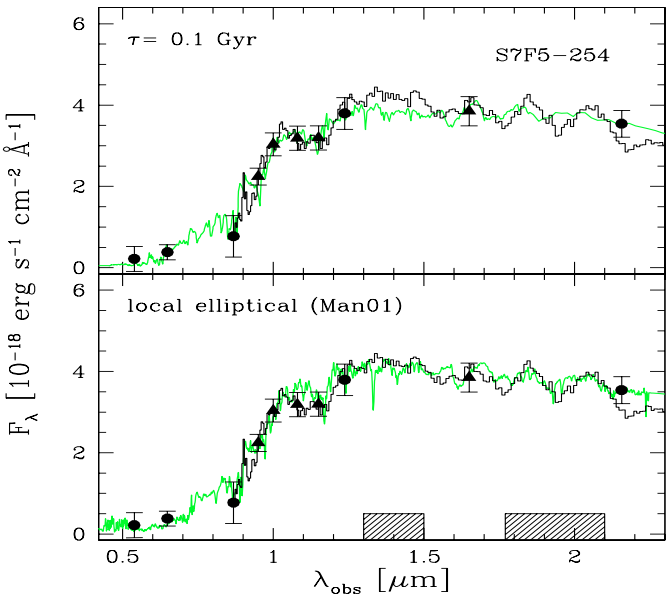

Fig. 4. *Upper panel*: the best fitting template (thick grey line) is superimposed on the observed smoothed spectrum (thin black histogram) of S7F5_254. The filled circles are the photometric data in the V, R, I, J and K' bands from the MUNICS survey. The filled triangles are the additional photometric points derived by the observed spectrum (see Sect. 4 for details). *Lower panel*: the mean observed spectrum of local ellipticals (Mannucci et al. 2001, Man01) is superimposed on the observed smoothed spectrum of S7F5_254. Symbols are as in the upper panel.

good fit ($P(\tilde{\chi}^2) \simeq 0.95$). In this case we obtain a mean age of 0.5 Gyr and an extinction $A_V = 1.75$ mag. In Fig. 5 the best-fitting model, the observed spectrum and the photometric data relevant to S7F5_45 are shown (upper panel). These results suggest that the emission of this galaxy is dominated by a population of stars recently formed. On the other hand this population has to be formed in a burst with a time-scale much shorter than the mean age itself (i.e. $\tau \ll 0.5$ Gyr) otherwise we should obtain an acceptable fit also with $\tau \geq 1$ models. Unless to hypothesize that all the stellar mass of this galaxy is formed in such a short burst, the population of stars recently formed has to be superimposed to an older population. This is quantitatively shown in Fig. 5 (lower panel) where a composite stellar population (CSP) is superimposed to the data. The CSP shown is the weighted sum of the best-fitting SSP and an old (5 Gyr, $\tau = 1$, $Z = Z_\odot$, $A_V = 0$) template spectrum. They have been weighted so that the old spectrum contribute for 60% of the total stellar mass. It is evident that the population of stars recently formed dominates the emission even in this extreme case. Thus, the stellar mass-to-light ratio relevant to a mean age of 0.5 Gyr represents the most "conservative" choice we can make. The lowest ratio for this mean age is ∼0.15 $M_\odot/L_\odot$, the value given by the Miller-Scalo IMFs (e.g. Fig. 2). Given the K-band absolute magnitude of S7F5_45 resulting from the fitting models ($M_K = -27.7$) we derive a minimum stellar mass $\mathcal{M}^{\rm min}_{\rm stars} = 4 \times 10^{11}\ M_\odot$. For this galaxy, the best-fitting model requires a lower limit to the formation redshift $z_{\rm f} \gtrsim 2$.

5. Summary and conclusions

We have presented low resolution near-IR spectra of two candidates $z > 1$ massive ($\mathcal{M}_{\rm stars} > 10^{11}\ M_\odot$) galaxies out of the 15 candidates selected from the MUNICS survey ($R - K > 5$ and $K < 18$). The spectra, obtained with NICS-Amici, place the two EROs at $1.2 < z < 1.5$. The stellar mass derived by their rest-frame $z = 1.2$ K-band absolute magnitude ($M_K \simeq -26.6$) and assuming the local stellar mass-to-light ratio ($0.73\ M_\odot/L_\odot$) is $\mathcal{M}_{\rm stars} \sim 7 \times 10^{11}\ M_\odot$. In order to better constrain the redshift and to obtain a lower limit to the stellar mass we have compared the spectra and the photometric data with a set of template spectra by means of a $\tilde{\chi}^2$ best-fitting procedure. The best-fit to the

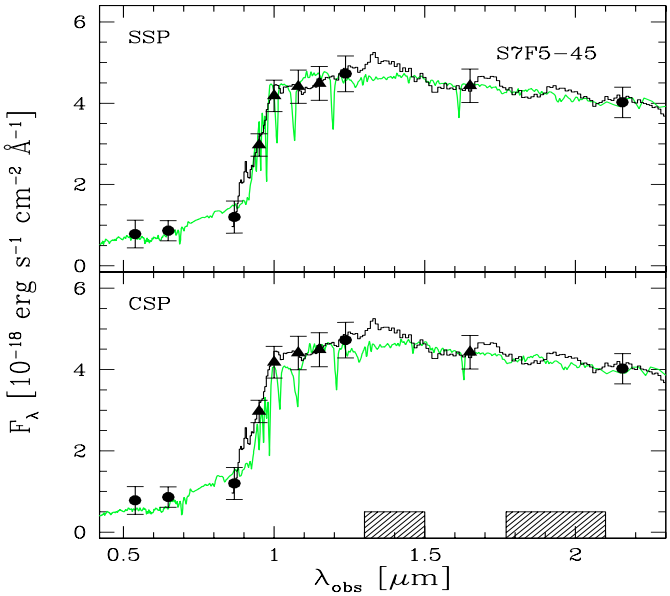

Fig. 5. *Upper panel*: the best fitting template (thick grey line) is superimposed on the observed smoothed spectrum (thin black histogram) of S7F5_45. Symbols are as in Fig. 4. *Lower panel*: a composite stellar population (CSP) is superimposed to the data. The CSP is the weighted sum of the best-fitting SSP and an old (5 Gyr, $\tau = 1$, $Z = Z_\odot$, $A_V = 0$) template spectra. They have been weighted so that the old component contribute 60% of the total stellar mass.

data provides a redshift $z \simeq 1.22$ for S7F5_254 and $z \simeq 1.46$ for S7F5_45. We estimate a lower limit to their stellar mass of $\mathcal{M}^{\rm min}_{\rm stars} = 6 \times 10^{11}\ M_\odot$ and $\mathcal{M}^{\rm min}_{\rm stars} = 4 \times 10^{11}\ M_\odot$ respectively, under the most conservative results provided by the best-fitting models. Thus, these two galaxies are among the most luminous and massive evolved galaxies detected so far at redshift $z > 1$. The galaxy S7F5_254 is comparatively older than S7F5_45. The youngest mean ages of the population of stars dominating the emission of the two EROs are 3.5 Gyr and 0.5 Gyr respectively which suggest formation redshift of $z_{\rm f} \gtrsim 3.5$ and $z_{\rm f} \gtrsim 2$. These results, even if limited to two EROs, point to a galaxy formation scenario where massive evolved galaxies are already well in place at $z \gtrsim 1.5$. Given the high values of the lower limit to the $\mathcal{M}_{\rm stars}$ of our EROs, they could severely constrain the galaxy formation models. Spectrophotometric models of galaxies with an accurate modeling of the horizontal branch and including different values of α/Fe (Maraston & Thomas 2000; Thomas et al. 2002) as well as the emission from the gas component (Charlot & Longhetti 2001), will allow us to interpret the higher resolution near-IR spectroscopic data we expect in the next spring at VLT-ISAAC. These data make it possible to restrict the ranges of ages and metallicity providing a more accurate estimate of the stellar mass of the two massive galaxies presented here. Moreover, our XMM observations scheduled in 2003 will allow us to put severe constraints on the presence of AGNs in early-type galaxies at high redshifts.

Acknowledgements. We would like to thank E. Oliva for the useful discussions and suggestions relevant to the Amici spectra. We also thank the anonymous referee for his comments, which helped to improve the presentation of the paper. PS acknowledge financial support by the Italian *Consorzio Nazionale per l'Astronomia e l'Astrofisica* (CNAA). RB, ND, GF and UH acknowledge support by the SFB 375 of the Deutsche Forschungsgemeinschaft.

References

Allen, C. W. 1973, Astrophysical Quantities (Athlon Press, London)
Baugh, C. M., Benson, A. J., Cole, S., Frenk, C. S., & Lacey, C. 2002 [astro-ph/0203051]
Benitez, N., Broadhurst, T., Bouwens, R., Silk, J., & Rosati, P. 1999, ApJ, 515, L68
Bolzonella, M., Miralles, J.-M., & Pellò, R. 2000, A&A, 363, 476
Bruzual, A. G., & Charlot, S. 1993, ApJ, 405, 538
Bruzual, A. G., & Kron, R. G. 1980, ApJ, 241, 25
Calzetti, D., Armus, L., Bohlin, R. C., et al. 2000, ApJ, 533, 68
Charlot, S., & Longhetti, M. 2001, MNRAS, 323, 887
Cimatti, A., Daddi, E., di Serego Alighieri, S., et al. 1999, A&A, 352, L45
Cimatti, A., Daddi, E., Mignoli, M., et al. 2002, A&A, 381, L68
Cole, S., Lacey, C. G., Baugh, C. M., & Frenk, C. S. 2000, MNRAS, 319, 168
Cole, S., Norberg, P., Baugh, C. M., et al. 2001, MNRAS, 326, 255
Daddi, E., Cimatti, A., Pozzetti, L., et al. 2000, A&A, 361, 535
Dey, A., Graham, J. R. I., Rob, J., et al., ApJ, 519, 610
Drory, N., Feulner, G., Bender, R., et al. 2001, MNRAS, 325, 550
Falco, E. E., Kurtz, M. J., Geller, M. J., et al. 1999, PASP, 111, 438
Franceschini, A., Silva, L., Fasano, G., et al. 1998, AJ, 506, 600
Hunt, L. K., Mannucci, F., Testi, L., Migliorini, S., Stanga, R. M., Baffa, C., Lisi, F., & Vanzi, L. 2000, AJ, 119, 985
Jimenez, R., Friaca, A. C. S., Dunlop, J. S., et al. 1999, MNRAS, 305, L16
Kauffmann, G. 1996, MNRAS, 281, 487
Kauffmann, G., & Charlot, S. 1998, MNRAS, 297, L23
Kinney, A. L., Calzetti, D., Bohlin, R. C., et al. 1996, ApJ, 467, 38
Mannucci, F., Pozzetti, L., Thompson, D., et al. 2002, MNRAS, 329, L57
Mannucci, F., Basile, F., Poggianti, B. M., et al. 2001, MNRAS, 326, 745
Maraston, C., & Thomas, D. 2000, ApJ, 541, 126
Martini, P. 2001, AJ, 121, 2301
McCarthy, P. J., Carlberg, R. G., Chen, H.-W, et al. 2001, ApJ, 560, L131
Oliva, E. 2001, Mem. Sc. Astr. It., in press [astro-ph/0102427]
Peebles, P. J. E. 2001, ASP Conf. Ser., in press [astro-ph/0201015]
Pozzetti, L., & Mannucci, F. 2000, MNRAS, 317, L17
Renzini, A., & Cimatti, A. 1999, ASP Conf. Ser., 193, ed. A. J. Bunker, & W. J. M. van Breugel, 312
Roche, N. D., Almaini, O., Dunlop, J., Ivison, R. J., & Willott, C. J. 2002, MNRAS [astro-ph/0205259]
Rosati, P., Stanford, A., Lidman, C., Mainieri, V., & Eisenhardt, P. 2000, Deep Fields, ed. S. Cristiani, A. Renzini, & R. E. Williams (Springer)
Saracco, P., Longhetti, M., Severgnini, P., et al. 2002, Galaxy Evolution: Theory and Observations, ed. V. Avila-Reese, C. Firmani, C. Frenk, & C. Allen, Rev. Mex. Astron. Astrofis. SC [astro-ph/0207352]
Scodeggio, M., & Silva, D. R. 2000, A&A, 359, 953
Schmitt, H. R., Kinney, A. L., Calzetti, D., & Storchi-Bergmann, T. 1997, AJ, 114, 592
Soifer, B. T., Matthews, K., Neugebauer, G., et al. 1999, ApJ, 118, 2065
Stiavelli, M., Treu, T., Carollo, C. M., et al. 1999, A&A, 343, L25
Thomas, D., Maraston, C., & Bender, R. 2002, Ap&SS, 281, 371
Thompson, D., Beckwith, S. V. W., Fockenbrock, R., et al. 1999, ApJ, 523, 100
Tinsley, B. M. 1972, ApJ, 178, 319
van Dokkum, P. G., & Stanford, S. A. 2001, ApJ, 562, L35